

# Dynamical properties of an exactly solvable coupled quantum double-well system: The evolution speed and entanglement

Hideo Hasegawa\*

*Department of Physics, Tokyo Gakugei University, Koganei, Tokyo 184-8501, Japan*

(Dated: August 18, 2021)

## Abstract

We have studied dynamical properties of an exactly solvable quantum coupled double-well (DW) system with Razavy's hyperbolic potential. With the use of four kinds of initial wavepackets, the correlation function  $\Gamma(t)$  and the concurrence  $C(t)$  which is a typical measure of the entanglement in two qubits, are calculated. We obtain the orthogonality time  $\tau$  which signifies a time interval for an initial state to evolve to its orthogonal state, and the temporal average of  $C_{av}$  ( $= \sqrt{\langle C(t)^2 \rangle}$ ). The coupling dependence of  $\tau$  and the concurrence [ $C_{av}$  or  $C(0)$ ], and the relation between  $\tau$  and the concurrence are investigated. Our calculations have shown that the evolution speed measured by  $\tau^{-1}$  is not necessarily increased with increasing the concurrence in coupled DW systems.

Keywords: coupled double-well potential, Razavy's potential, evolution speed, entanglement

PACS numbers: 03.65.-w, 03.67.Mn

---

\*hideohasegawa@goo.jp

## I. INTRODUCTION

The two-level (TL) system has been employed for a study on qubits which play important roles in quantum information and quantum computation [1]. The connection between the quantum evolution speed and the entanglement has been extensively studied with the use of the TL model [2–10]. It has been pointed out that the speed of evolution in certain quantum state may be measured by the orthogonality time which expresses a time for an initial state to reach its orthogonal state [2–5]. Margolus and Levitin [2] asserted that the orthogonal time  $\tau$  is given by  $\tau \geq \pi\hbar/(2E)$  where  $E$  stands for the expectation energy of a given quantum system relative to the ground-state energy. This result complements the time-energy uncertainty relation requiring  $\tau \geq \pi\hbar/(2\Delta E)$  where  $\Delta E$  expresses the root-mean-square value of the system energy [3]. Combining the above two results [2, 3], Giovannetti *et al.* [4, 5] pointed out that the entanglement permits to achieve the maximum evolution speed measured by  $\tau_{\min}$  which is given by

$$\tau \geq \tau_{\min} \equiv \max\left(\frac{\pi\hbar}{2E}, \frac{\pi\hbar}{2\Delta E}\right). \quad (1)$$

Batle *et al.* [6] and Curilef *et al.* [7] showed that in two uncoupled qubits, the ratio of  $\tau/\tau_{\min}$  is unity for a maximally entangled state and  $\sqrt{2}$  for a separate state [6, 7]. Borrás *et al.* [8] made an extension of Ref. [6] for two uncoupled qubits, showing a clear correlation between the evolution speed and concurrence. It was pointed out by Chau [9] that for the singular case with  $|a_3|^2 = 0$  which was not discussed in Refs. [6, 8], the relation between entanglement and  $\tau$  can be very different from the generic case with  $|a_3|^2 \neq 0$ , where  $a_3$  means the expansion coefficient in a wavepacket [Eq. (24)]. A concept of the orthogonality time is generalized to the case where an initial state evolves to an arbitrary final state [5, 8]. Effects of interactions between two qubits which modify the entanglement are investigated in Refs. [4, 10]. Zander *et al.* [10] have made a detailed study on the relation between the ratio of  $\tau/\tau_{\min}$  and the entanglement in interacting two qubits. It is shown that, with the exception of some marginal special cases, only initial states with low entanglement tend to evolve in the fastest way in coupled qubits [10]. Related discussion will be given in Sec. IV.

Double-well (DW) potential models have been widely employed in various fields of quantum physics. Although quartic DW potentials are commonly adopted for the theoretical study, one cannot obtain their exact eigenvalues and eigenfunctions of the Schrödinger equation. Then it is necessary to apply various approximate approaches such as perturbation and

spectral methods to quartic potential models [11]. Razavy [12] proposed the quasi-exactly solvable hyperbolic DW potential, for which one may exactly determine a part of whole eigenvalues and eigenfunctions. A family of quasi-exactly solvable potentials has been investigated [13, 14]. In contrast to the TL model which is a simplified model of a DW system, studies on *coupled* DW systems are scanty, as far as we are aware of. This is because a calculation of a coupled DW system is much tedious than those of a single DW system and of a coupled TL model. In the present study, we adopt coupled two DW systems, each of which is described by Razavy's potential. One of advantages of our model is that we may exactly determine eigenvalues and eigenfunctions of the coupled DW system. We study dynamics of wavepackets, calculating the correlation function  $\Gamma(t)$  by which the orthogonality time  $\tau$  is obtained, and the concurrence  $C(t)$  which is one of typical measures of entanglement. We investigate the relation between the speed of quantum evolution measured by  $\tau^{-1}$  and the entanglement expressed by the concurrence. The difference and similarity between results in our coupled DW system and the TL model [4–8, 10] are discussed. These are purposes of the present paper.

The paper is organized as follows. In Sec. II, we describe the calculation method employed in our study, briefly explaining Razavy's potential [12]. Exact analytic expressions for eigenvalues and eigenfunctions for coupled DW systems are presented. In Sec. III, with the use of four kinds of initial wavepackets, we perform model calculations of the time-dependent correlation  $\Gamma(t)$  and concurrence  $C(t)$ , evaluating the orthogonality time  $\tau$  and temporal average of concurrence  $C_{av}$  ( $= \sqrt{\langle C(t)^2 \rangle}$ ). The relation between the calculated  $\tau$  and the concurrence,  $C_{av}$  or  $C(0)$ , is studied. Sec. IV is devoted to our conclusion.

## II. THE ADOPTED METHOD

### A. Coupled double-well system with Razavy's potential

We consider coupled two DW systems whose Hamiltonian is given by

$$H = \sum_{n=1}^2 \left[ -\frac{\hbar^2}{2m} \frac{\partial^2}{\partial x_n^2} + V(x_n) \right] - gx_1x_2, \quad (2)$$

with

$$V(x) = \frac{\hbar^2 \kappa^2}{2m} \left[ \frac{\xi^2}{8} \cosh 4\kappa x - 4\xi \cosh 2\kappa x - \frac{\xi^2}{8} \right], \quad (3)$$

where  $x_1$  and  $x_2$  stand for coordinates of two distinguishable particles of mass  $m$  in double-well systems coupled by an interaction  $g$ , and Razavy's potential  $V(x)$  depends on two parameters of  $\xi$  and  $\kappa$  [12]. The potential  $V(x)$  with  $\hbar = m = \xi = \kappa = 1.0$  adopted in this study is plotted in Fig. 1(a). Minima of  $V(x)$  locate at  $x_s = \pm 1.38433$  with  $V(x_s) = -8.125$  and its maximum is  $V(0) = -2.0$  at  $x = 0.0$  [15].

First we consider the case of  $g = 0.0$  in Eqs. (2) and (3). Eigenvalues of Razavy's double-well potential of Eq. (3) are given by [12]

$$\epsilon_0 = \frac{1}{2} \left[ -\xi - 5 - 2\sqrt{4 - 2\xi + \xi^2} \right], \quad (4)$$

$$\epsilon_1 = \frac{1}{2} \left[ \xi - 5 - 2\sqrt{4 + 2\xi + \xi^2} \right], \quad (5)$$

$$\epsilon_2 = \frac{1}{2} \left[ -\xi - 5 + 2\sqrt{4 - 2\xi + \xi^2} \right], \quad (6)$$

$$\epsilon_3 = \frac{1}{2} \left[ \xi - 5 + 2\sqrt{4 + 2\xi + \xi^2} \right]. \quad (7)$$

Eigenvalues for the adopted parameters are  $\epsilon_0 = -4.73205$ ,  $\epsilon_1 = -4.64575$ ,  $\epsilon_2 = -1.26795$  and  $\epsilon_3 = 0.645751$ . Both  $\epsilon_0$  and  $\epsilon_1$  locate below  $V(0)$  as shown by dashed curves in Fig. 1(a), and  $\epsilon_2$  and  $\epsilon_3$  are far above  $\epsilon_1$ . In this study, we take into account the lowest two states of  $\epsilon_0$  and  $\epsilon_1$  whose eigenfunctions are given by [12]

$$\phi_0(x) = A_0 e^{-\xi \cosh 2x/4} \left[ 3\xi \cosh x + (4 - \xi + 2\sqrt{4 - 2\xi + \xi^2}) \cosh 3x \right], \quad (8)$$

$$\phi_1(x) = A_1 e^{-\xi \cosh 2x/4} \left[ 3\xi \sinh x + (4 + \xi + 2\sqrt{4 + 2\xi + \xi^2}) \sinh 3x \right], \quad (9)$$

$A_n$  ( $n = 0, 1$ ) denoting normalization factors. Figure 1(b) shows the eigenfunctions of  $\phi_0(x)$  and  $\phi_1(x)$ , which are symmetric and anti-symmetric, respectively, with respect to the origin.

## B. Eigenvalues and eigenstates of the coupled DW system

We calculate exact eigenvalues and eigenstates of the coupled two DW systems described by Eq. (2). With basis states of  $\phi_0\phi_0$ ,  $\phi_0\phi_1$ ,  $\phi_1\phi_0$  and  $\phi_1\phi_1$  where  $\phi_n\phi_k \equiv \phi_n(x_1)\phi_k(x_2)$ , the energy matrix for the Hamiltonian given by Eq. (2) is expressed by

$$\mathcal{H} = \begin{pmatrix} 2\epsilon_0 & 0 & 0 & -g\gamma^2 \\ 0 & \epsilon_0 + \epsilon_1 & -g\gamma^2 & 0 \\ 0 & -g\gamma^2 & \epsilon_0 + \epsilon_1 & 0 \\ -g\gamma^2 & 0 & 0 & 2\epsilon_1 \end{pmatrix}, \quad (10)$$

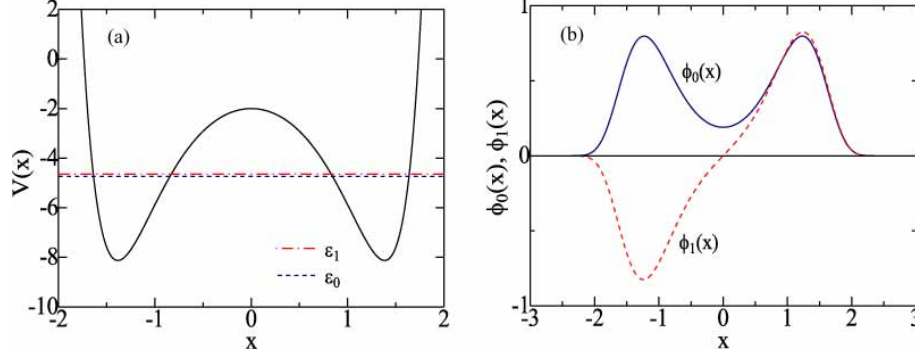


FIG. 1: (Color online) (a) Razavy's DW potential  $V(x)$  (solid curve), dashed and chain curves expressing eigenvalues of  $\epsilon_0$  and  $\epsilon_1$ , respectively, for  $\hbar = m = \xi = \kappa = 1.0$  [Eq.(3)]. (b) Eigenfunctions of  $\phi_0(x)$  (solid curve) and  $\phi_1(x)$  (dashed curve).

with

$$\gamma = \int_{-\infty}^{\infty} \phi_0(x) x \phi_1(x) dx = 1.13823. \quad (11)$$

Eigenvalues of the energy matrix are given by

$$E_0 = \epsilon - \sqrt{\delta^2 + g^2\gamma^4}, \quad (12)$$

$$E_1 = \epsilon - g\gamma^2, \quad (13)$$

$$E_2 = \epsilon + g\gamma^2, \quad (14)$$

$$E_3 = \epsilon + \sqrt{\delta^2 + g^2\gamma^4}, \quad (15)$$

where

$$\epsilon = \epsilon_1 + \epsilon_0 = -9.3778, \quad (16)$$

$$\delta = \epsilon_1 - \epsilon_0 = 0.0863. \quad (17)$$

Corresponding eigenfunctions are given by

$$\Phi_0(x_1, x_2) = \cos \theta \phi_0(x_1)\phi_0(x_2) + \sin \theta \phi_1(x_1)\phi_1(x_2), \quad (18)$$

$$\Phi_1(x_1, x_2) = \frac{1}{\sqrt{2}} [\phi_0(x_1)\phi_1(x_2) + \phi_1(x_1)\phi_0(x_2)], \quad (19)$$

$$\Phi_2(x_1, x_2) = \frac{1}{\sqrt{2}} [-\phi_0(x_1)\phi_1(x_2) + \phi_1(x_1)\phi_0(x_2)], \quad (20)$$

$$\Phi_3(x_1, x_2) = -\sin \theta \phi_0(x_1)\phi_0(x_2) + \cos \theta \phi_1(x_1)\phi_1(x_2), \quad (21)$$

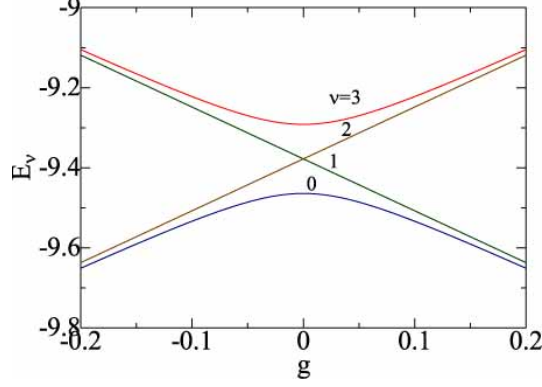


FIG. 2: (Color online) Eigenvalues  $E_\nu$  ( $\nu = 0-3$ ) of a coupled DW system as a function the coupling strength  $g$ .

where

$$\tan 2\theta = \frac{g\gamma^2}{\delta}. \quad \left(-\frac{\pi}{4} \leq \theta \leq \frac{\pi}{4}\right) \quad (22)$$

Eigenvalues  $E_\nu$  ( $\nu = 0-3$ ) are plotted as a function of  $g$  in Fig. 2, which is symmetric with respect to  $g = 0.0$ . For  $g = 0.0$ ,  $E_1$  and  $E_2$  are degenerate. We hereafter study the case of  $g \geq 0.0$ . With increasing  $g$ , energy gaps between  $E_0$  and  $E_1$  and between  $E_2$  and  $E_3$  are gradually decreased while that between  $E_1$  and  $E_2$  is increased. We note that differences between eigenvalues defined by  $\Omega_\nu = (E_\nu - E_0)/\hbar$  satisfy the relation:

$$\Omega_3 = \Omega_1 + \Omega_2. \quad (23)$$

For  $g = 0.0$ , we obtain  $\Omega_1 = \Omega_2 = \Omega_3/2$ .

### C. The correlation function and orthogonality time

The time-dependent wavepacket is expressed by

$$\Psi(t) = \Psi(x_1, x_2, t) = \sum_{\nu=0}^3 a_\nu \Phi_\nu(x_1, x_2) e^{-iE_\nu t/\hbar}, \quad (24)$$

where expansion coefficients  $a_\nu$  satisfy the relation

$$\sum_{\nu=0}^3 |a_\nu|^2 = 1. \quad (25)$$

The correlation function  $\Gamma(t)$  is defined by

$$\Gamma(t) = \left| \int_{-\infty}^{\infty} \int_{-\infty}^{\infty} \Psi^*(x_1, x_2, 0) \Psi(x_1, x_2, t) dx_1 dx_2 \right|, \quad (26)$$

$$= \left| |a_0|^2 + \sum_{\nu=1}^3 |a_\nu|^2 e^{-i\Omega_\nu t} \right|. \quad (27)$$

The orthogonality time  $\tau$  is provided by a time interval such that an initial wavepacket takes to evolve into the orthogonal state [4–7],

$$\tau = \min_{\forall t > 0} \{\Gamma(t) = 0\}. \quad (28)$$

In the case of wavepackets including only two states with  $a_\nu = (1/\sqrt{2}) (\delta_{\nu,0} + \delta_{\nu,\kappa})$ , the correlation function becomes

$$\Gamma(t) = \frac{1}{2} |1 + e^{-i\Omega_\kappa t}| = \sqrt{\frac{1 + \cos \Omega_\kappa t}{2}}, \quad (29)$$

for which we easily obtain  $\tau$

$$\tau = \frac{\pi}{\Omega_\kappa}. \quad (30)$$

In the case of  $g = 0.0$ , Eq. (28) becomes

$$\tau = \min_{\forall t} \{|a_0|^2 + (|a_1|^2 + |a_2|^2) z(t) + |a_3|^2 z(t)^2 = 0\}, \quad (31)$$

where  $z(t) = e^{-i\Omega_1 t}$ . Solutions of  $\tau$  may be obtainable from roots of respective polynomial equations for  $z(t)$  [6–8]. In a general case, however,  $\tau$  is obtainable by solving Eq. (28) with a numerical method.

#### D. The concurrence

We have calculated the concurrence of coupled DW systems. Substituting Eqs. (18)-(21) into Eq. (24), we obtain

$$|\Psi\rangle = c_{00}|0\ 0\rangle + c_{01}|0\ 1\rangle + c_{10}|1\ 0\rangle + c_{11}|1\ 1\rangle, \quad (32)$$

with

$$c_{00} = a_0 \cos \theta e^{-iE_0 t} - a_3 \sin \theta e^{-iE_3 t}, \quad (33)$$

$$c_{01} = \frac{1}{\sqrt{2}} (a_1 e^{-iE_1 t} - a_2 e^{-iE_2 t}), \quad (34)$$

$$c_{10} = \frac{1}{\sqrt{2}} (a_1 e^{-iE_1 t} + a_2 e^{-iE_2 t}), \quad (35)$$

$$c_{11} = a_0 \sin \theta e^{-iE_0 t} + a_3 \cos \theta e^{-iE_3 t}, \quad (36)$$

where  $|k \ell\rangle = \phi_k(x_1)\phi_\ell(x_2)$  with  $k, \ell = 0, 1$ . The concurrence  $C$  of the state  $|\Psi\rangle$  given by Eq. (32) is defined by [16]

$$C^2 = 4 |c_{00}c_{11} - c_{01}c_{10}|^2. \quad (37)$$

The state given by Eq. (32) becomes factorizable if and only if the relation:  $c_{00}c_{11} - c_{01}c_{10} = 0$  holds. Substituting Eqs. (33)-(36) into Eq. (37), we obtain the concurrence

$$C(t)^2 = |(a_0^2 - a_3^2 e^{-2i\Omega_3 t}) \sin 2\theta + 2a_0 a_3 \cos 2\theta e^{-i\Omega_3 t} - a_1^2 e^{-2i\Omega_1 t} + a_2^2 e^{-2i\Omega_2 t}|^2, \quad (38)$$

whose initial value becomes

$$C(0)^2 = |(a_0^2 - a_3^2) \sin 2\theta + 2a_0 a_3 \cos 2\theta - a_1^2 + a_2^2|^2. \quad (39)$$

We should note that the concurrence becomes time dependent in general for  $g \neq 0.0$  because the coupling modifies the entanglement in two qubits, although it is time-independent for uncoupling case ( $g = 0.0$ ) where  $\theta = 0.0$  and  $\Omega_1 = \Omega_2 = \Omega_3/2$ .

### III. MODEL CALCULATIONS AND DISCUSSION

#### A. Adopted wavepackets

There are many possibilities in choosing expansion coefficients  $a_\nu$  ( $\nu = 0 - 3$ ) of a wavepacket which satisfy Eq. (25). Among them, we have studied in this paper, the four wavepackets A-D whose expansion coefficients are listed in Table 1.

wavepacket	$a_0$	$a_1$	$a_2$	$a_3$
A	$\frac{1}{2}$	$\frac{1}{\sqrt{2}}$	0	$\frac{1}{2}$
B	$\frac{1}{\sqrt{2}}$	0	0	$\frac{1}{\sqrt{2}}$
C	$\frac{1}{\sqrt{2}}$	$\frac{1}{\sqrt{2}}$	0	0
D	$\frac{1}{2}$	$\frac{1}{2}$	$\frac{1}{2}$	$\frac{1}{2}$

*Table 1* Assumed expansion coefficients  $a_\nu$  ( $\nu = 0$  to 3) for four wavepackets A, B, C and D.



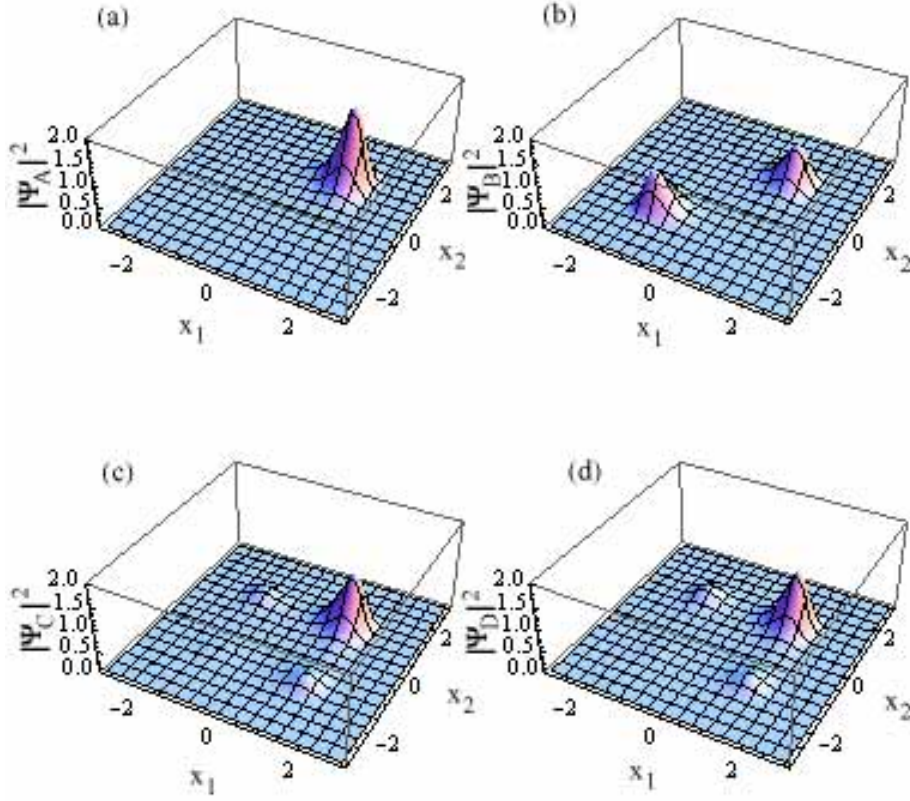


FIG. 3: (Color online) Magnitudes  $|\Psi(x_1, x_2)|^2$  of adopted four wavepackets of (a) A, (b) B, (c) C and (d) D for  $g = 0.0$  at  $t = 0.0$ .

Coefficients in adopted wavepackets A-D are chosen as follows: A factorizable product state for  $g = 0.0$  is expressed by

$$\Psi_{prod} = \Psi_R(x_1)\Psi_R(x_2), \quad (40)$$

$$= \frac{1}{2} [\phi_0(x_1)\phi_0(x_2) + \phi_0(x_1)\phi_1(x_2) + \phi_1(x_1)\phi_0(x_2) + \phi_1(x_1)\phi_1(x_2)], \quad (41)$$

$$= \frac{1}{2} [\Phi_0(x_1, x_2) + \Phi_3(x_1, x_2)] + \frac{1}{\sqrt{2}} \Phi_1(x_1, x_2), \quad (42)$$

where magnitude of  $\Psi_R(x_\nu)$  ( $= [\phi_0(x_\nu) + \phi_1(x_\nu)]/\sqrt{2}$ ) localizes at the right well in the  $x_\nu$  axis ( $\nu = 1, 2$ ). The wavepacket yielding initially the product state given by Eq. (42) is described by the wavepacket A with  $a_0 = a_3 = 1/2$  and  $a_1 = 1/\sqrt{2}$ .

As a typical entangled state which cannot be expressed in a factorized form, we consider the state for  $g = 0.0$ ,

$$\Psi_{ent}(x_1, x_2) = \frac{1}{\sqrt{2}} [\phi_0(x_1)\phi_0(x_2) + \phi_1(x_1)\phi_1(x_2)], \quad (43)$$

$$= \frac{1}{\sqrt{2}} [\Phi_0(x_1, x_2) + \Phi_3(x_1, x_2)]. \quad (44)$$

The relevant wavepacket is expressed by the wavepacket B with  $a_0 = a_3 = 1/\sqrt{2}$ .

The wavepacket C consists of the ground and first-excited states with  $a_0 = a_1 = 1/\sqrt{2}$ , which has been commonly adopted as a wavepacket. The wavepacket D includes four components with equal weights of  $a_\nu = 1/2$  for  $\nu = 0 - 3$ .

Figures 3(a), 3(b), 3(c) and 3(d) show magnitudes  $|\Psi(x_1, x_2)|^2$  of wavepackets A, B, C and D, respectively, for  $g = 0.0$  at  $t = 0.0$  generated by Eq. (24) with expansion coefficients shown in Table 1. The wavepacket A has a peak at the RR side in the  $(x_1, x_2)$  space while the wavepacket B has two peaks at RR and LL sides, where *RR* (*LL*) signifies the right (left) side in the  $x_1$  axis and the right (left) side in  $x_2$  axis. Wavepackets C and D have similar profiles with main peaks at the RR side at  $t = 0.0$  for  $g = 0.0$ , but they are quite different at  $t \neq 0.0$  or for  $g \neq 0.0$  (compare Figs. 8 and 9 with Figs. 10 and 11, respectively). Wavepackets A, B, C and D which are initially localized in the  $(x_1, x_2)$  space are expected to be meaningful among conceivable wavepackets.

## B. Dynamics of $\Gamma(t)$ and $C(t)$

We will study dynamics of  $\Gamma(t)$  and  $C(t)$  for wavepackets A, B, C and D, which are separately described in subsections 1, 2, 3 and 4, respectively [15].

### 1. Wavepacket A: $a_0 = 1/2$ , $a_1 = 1/\sqrt{2}$ , $a_2 = 0$ and $a_3 = 1/2$

From Eq. (27) and expansion coefficients in Table 1, the correlation function of the wavepacket A is given by

$$\Gamma_A = \left| \frac{1}{2}e^{-i\Omega_1 t} + \frac{1}{4}(1 + e^{-i\Omega_3 t}) \right|. \quad (45)$$

Figure 4(a) shows the correlation function  $\Gamma_A(t)$  calculated for  $g = 0.0$  which yields  $\tau = 36.40$ . Figures 4(b) and 4(c) show  $\Gamma_A(t)$  with  $g = 0.1$  and  $0.2$ , respectively, which oscillate

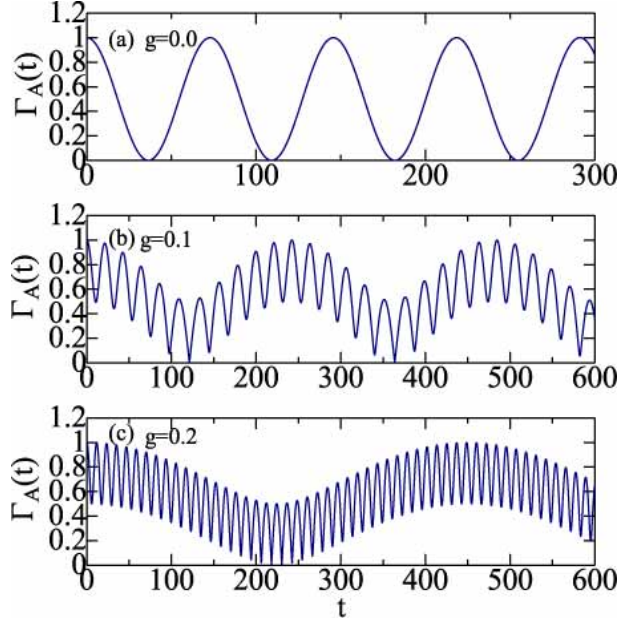


FIG. 4: (Color online) Correlation function  $\Gamma_A(t)$  for the wavepacket A with (a)  $g = 0.0$ , (b)  $g = 0.1$  and (c)  $g = 0.2$ .

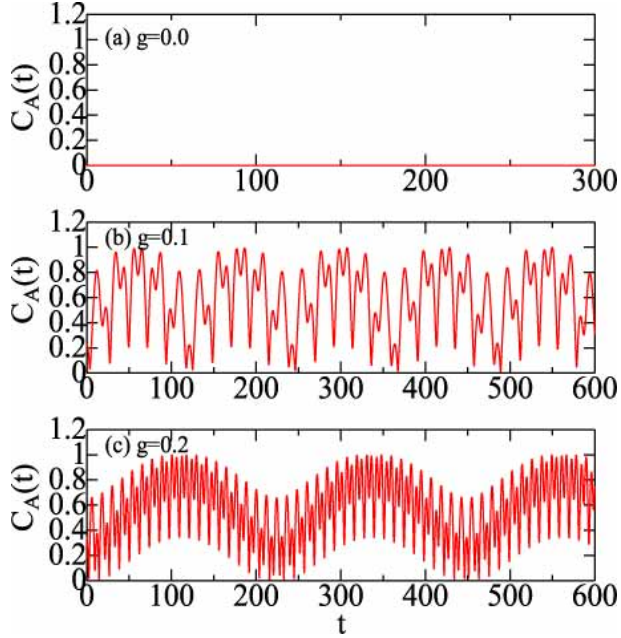


FIG. 5: (Color online) Concurrence  $C_A(t)$  for the wavepacket A with (a)  $g = 0.0$ , (b)  $g = 0.1$  and (c)  $g = 0.2$ ,  $C_A(t)$  being vanishing in (a).

more rapidly than that with  $g = 0.0$  in Fig. 4(a). However, the orthogonality times for  $g = 0.1$  and  $0.2$  are given by  $\tau = 121.0$  and  $218.8$ , respectively, which are larger than that for  $g = 0.0$  (36.40).

From Eq. (38), the concurrence of the wavepacket A is given by

$$C_A(t)^2 = \frac{1}{16} |2 e^{-2i\Omega_1 t} - 2 \cos 2\theta e^{-i\Omega_3 t} - \sin 2\theta (1 - e^{-2i\Omega_3 t})|^2, \quad (46)$$

which reduces to

$$C_A(0)^2 = \frac{1}{4} (1 - \cos 2\theta)^2. \quad (47)$$

Figure 5(a) shows that  $C_A(t)$  for  $g = 0.0$  is vanishing independently of time. We note in Figs. 5(b) and 5(c) that when the coupling is introduced,  $C_A(t)$  with initial values of  $C_A(0) = 0.223$  and  $0.342$  for  $g = 0.1$  and  $0.2$ , respectively, show complex time dependence which arises from a superposition of multiple contributions with frequencies of  $\Omega_1$ ,  $\Omega_3$ ,  $\Omega_3 - \Omega_1$  and  $\Omega_3 - 2\Omega_1$ .

The temporal average of  $\langle C_A(t)^2 \rangle$  may be analytically calculated as

$$\begin{aligned} C_{av}^2 = \langle C_A(t)^2 \rangle &= \frac{1}{8} (4 - \sin^2 2\theta) && \text{for } g > 0.0, \\ &= 0 && \text{for } g = 0.0. \end{aligned} \quad (48)$$

Note that  $C_{av}^2$  has the discontinuity at  $g = 0.0$  where  $\Omega_3 - 2\Omega_1 = 0$  (Fig. 2) [17]. We obtain  $C_{av} = 0.0, 0.707, 0.643$  and  $0.622$  for  $g = 0, 0_+, 0.1$  and  $0.2$ , respectively, where  $0_+ = \lim_{\epsilon \rightarrow 0} 0 + \epsilon$ .

## 2. Wavepacket B: $a_0 = 1/\sqrt{2}$ , $a_1 = a_2 = 0.0$ and $a_3 = 1/\sqrt{2}$

The correlation function of the wavepacket B is given by

$$\Gamma_B(t) = \frac{1}{2} (1 + e^{-i\Omega_3 t}), \quad (49)$$

which leads to  $\tau = \pi/\Omega_3$ . Figures 6(a), 6(b) and 6(c) show  $\Gamma_B(t)$  for  $g = 0.0, 0.1$  and  $0.2$ , respectively, for which the orthogonality times are  $\tau = 18.2, 10.1$  and  $5.75$ .

The concurrence of the wavepacket B is expressed by

$$C_B(t)^2 = \frac{1}{4} |\sin 2\theta (1 - e^{-2i\Omega_3 t}) + 2 \cos 2\theta e^{-i\Omega_3 t}|^2, \quad (50)$$

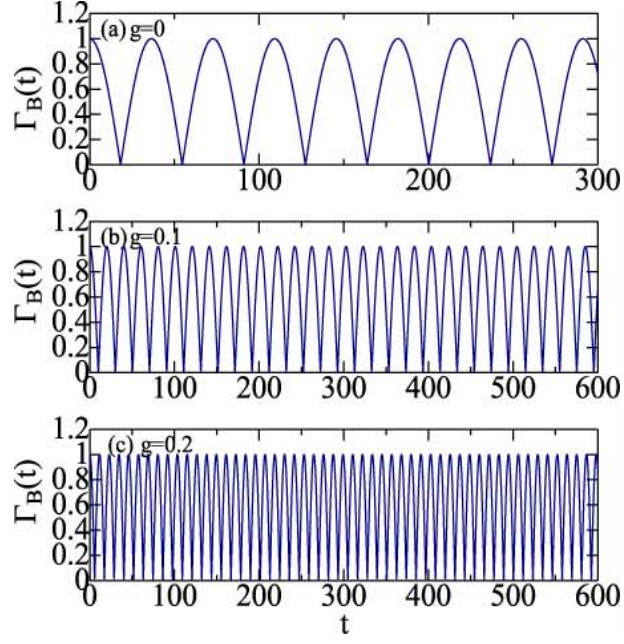


FIG. 6: (Color online) Correlation function  $\Gamma_B(t)$  for the wavepacket B with (a)  $g = 0.0$ , (b)  $g = 0.1$  and (c)  $g = 0.2$ .

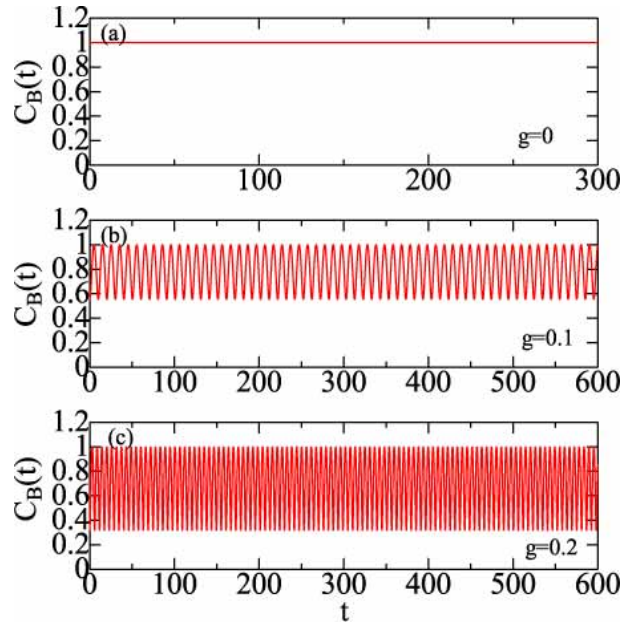


FIG. 7: (Color online) Concurrence  $C_B(t)$  for the wavepacket B with (a)  $g = 0.0$ , (b)  $g = 0.1$  and (c)  $g = 0.2$ .

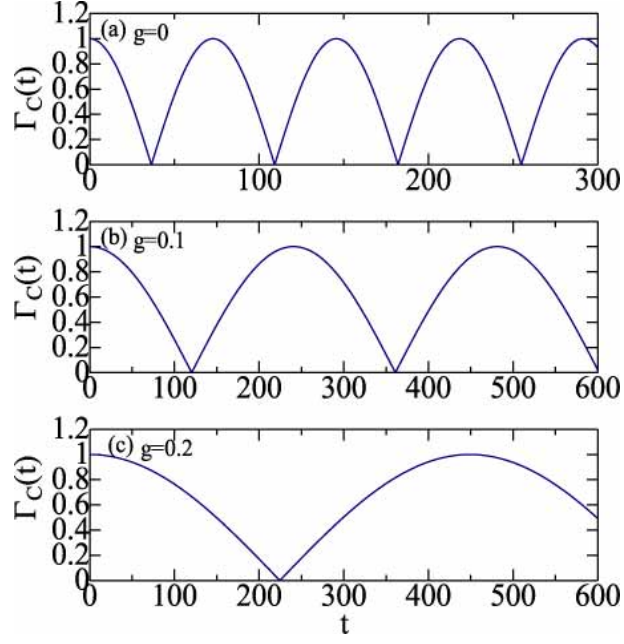


FIG. 8: (Color online) Correlation function  $\Gamma_C(t)$  for the wavepacket C with (a)  $g = 0.0$ , (b)  $g = 0.1$  and (c)  $g = 0.2$ .

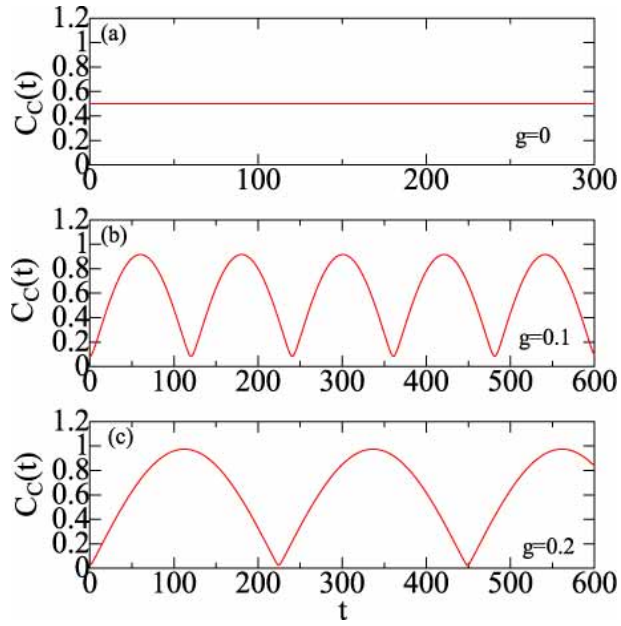


FIG. 9: (Color online) Concurrence  $C_C(t)$  for the wavepacket C with (a)  $g = 0.0$ , (b)  $g = 0.1$  and (c)  $g = 0.2$ .

with

$$C_B(0)^2 = \cos^2 2\theta, \quad (51)$$

from which we obtain  $C_B(0) = 1.0, 0.554$  and  $0.316$  for  $g = 0.0, 0.1$  and  $0.2$ , respectively. Calculated  $C_B(t)$  for  $g = 0.0, 0.1$  and  $0.2$  are plotted in Figs. 7(a), 7(b) and 7(c), respectively.  $C_B(t)$  for  $g = 0.0$  is unity independently of time. When the coupling  $g$  is introduced,  $C_B(t)$  becomes time dependent, showing rapid oscillations as shown in Figs. 7(b) and 7(c).

The temporal average of  $\langle C_B(t)^2 \rangle$  is given by

$$C_{av}^2 = \langle C_B(t)^2 \rangle = 1 - \frac{1}{2} \sin^2 2\theta, \quad (52)$$

which leads to  $C_{av} = 1.0, 0.808$  and  $0.742$  for  $g = 0.0, 0.1$  and  $0.2$ , respectively.

3. *Wavepacket C*:  $a_0 = a_1 = 1/\sqrt{2}$  and  $a_2 = a_3 = 0.0$

The correlation function of the wavepacket C is given by

$$\Gamma_C(t) = \frac{1}{2}(1 + e^{-i\Omega_1 t}), \quad (53)$$

leading to  $\tau = \pi/\Omega_1$ . Figures 8(a), 8(b) and 8(c) show  $\Gamma_C(t)$  for  $g = 0.0, 0.1$  and  $0.2$ , respectively, from which the orthogonality time is given by  $\tau = 36.40, 120.3$  and  $224.5$ .

The concurrence of the wavepacket C is expressed by

$$C_C(t)^2 = \frac{1}{4} |e^{-2i\Omega_1 t} - \sin 2\theta|^2, \quad (54)$$

which reduces to

$$C_C(0)^2 = \frac{1}{4}(1 - \sin 2\theta)^2. \quad (55)$$

We obtain  $C_C(0) = 0.5, 0.0839$  and  $0.0256$  for  $g = 0.0, 0.1$  and  $0.2$ , respectively. Figure 9(a) shows the time-independent  $C_C(t) = 0.5$  for  $g = 0.0$ . For  $g = 0.1$  and  $0.2$ ,  $C_C(t)$  show oscillations as shown in Figs. 9(b) and 9(b).

The temporal average is given by

$$C_{av}^2 = \langle C_C(t)^2 \rangle = \frac{1}{4}(1 + \sin^2 2\theta), \quad (56)$$

which yields  $C_{av} = 0.5, 0.651$  and  $0.689$  for  $g = 0.0, 0.1$  and  $0.2$ , respectively.



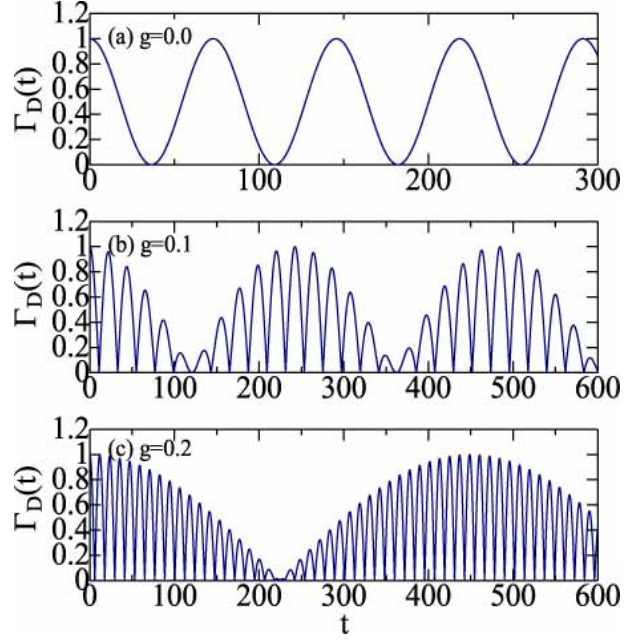


FIG. 10: (Color online) Correlation function  $\Gamma_D(t)$  for the wavepacket D with (a)  $g = 0.0$ , (b)  $g = 0.1$  and (c)  $g = 0.2$ .

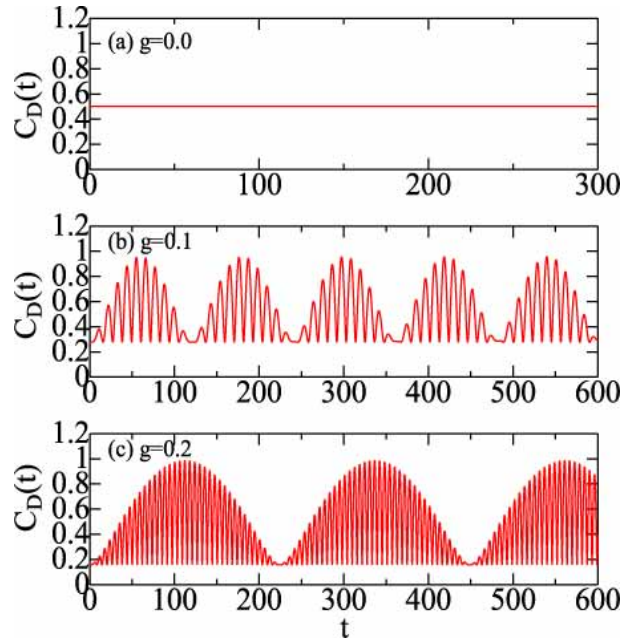


FIG. 11: (Color online) Concurrence  $C_D(t)$  for the wavepacket D with (a)  $g = 0.0$ , (b)  $g = 0.1$  and (c)  $g = 0.2$ .



4. *Wavepacket D*:  $a_0 = a_1 = a_2 = a_3 = 1/2$

The correlation function of the wavepacket D is expressed by

$$\Gamma_D(t) = \frac{1}{4} |1 + e^{-i\Omega_1 t} + e^{-i\Omega_2 t} + e^{-i\Omega_3 t}|, \quad (57)$$

$$= \frac{1}{4} |(1 + e^{-i\Omega_1 t})(1 + e^{-i\Omega_2 t})|, \quad (58)$$

where Eq. (23) is employed. For  $g = 0.0$ ,  $\Gamma_D(t)$  shows a simple sinusoidal oscillation because  $\Omega_1 = \Omega_2 = \Omega_3/2$  [Fig. 10(a)]. For  $g \neq 0.0$ , however,  $\Gamma_D(t)$  exhibits a rather complex oscillation as shown in Figs. 10(b) and 10(c), where  $\Gamma_D(t)$  vanishes at  $t = 36.40 (2k + 1)$ ,  $11.02 (2k + 1)$  and  $5.903 (2k + 1)$  for  $g = 0.0, 0.1$  and  $0.2$ , respectively, with  $k = 0, 1, 2, \dots$ . We obtain the orthogonality time expressed by  $\tau = \pi/\Omega_2$ , which leads to  $\tau = 36.40, 11.02$  and  $5.903$  for  $g = 0.0, 0.1$  and  $0.2$ , respectively.

The concurrence of the wavepacket D is given by

$$C_D(t)^2 = \frac{1}{16} |\sin 2\theta(1 - e^{-2i\Omega_3 t}) + 2 \cos 2\theta e^{-i\Omega_3 t} - e^{-2i\Omega_1 t} + e^{-2i\Omega_2 t}|^2, \quad (59)$$

with

$$C_D(0)^2 = \frac{1}{4} \cos^2 2\theta, \quad (60)$$

yielding  $C_D(0) = 0.5, 0.277$  and  $0.158$  for  $g = 0.0, 0.1$  and  $0.2$ , respectively. Although  $C_D(t)$  for  $g = 0.0$  is  $0.5$  independently of  $t$  in Fig. 11(a),  $C_D(t)$  for  $g = 0.1$  and  $0.2$  show complicated time dependence in Figs. 11(b) and 11(c), respectively.

The averaged concurrence is given by

$$C_{av}^2 = \langle C_D(t)^2 \rangle = \frac{1}{8} (3 - \sin^2 2\theta) \quad \text{for } g > 0.0, \quad (61)$$

$$= \frac{1}{4} \quad \text{for } g = 0.0, \quad (62)$$

where a discontinuity arises from the relation:  $\Omega_1 - \Omega_2 \rightarrow 0$  as  $g \rightarrow 0.0$  [17]. We obtain  $C_{av} = 0.5, 0.612, 0.537$  and  $0.512$  for  $g = 0, 0_+, 0.1$  and  $0.2$ , respectively.

Before closing the subsection of Sec. III B, it is worthwhile to make a closer look to the dynamical properties of wavefunctions. There is one kind of wavepackets which is orthogonal to the initial wavepacket A, B or C: for example,  $|\Psi_A(x_1, x_2, \tau(2k + 1))|^2$  with  $k = 0, 1, 2, \dots$  has a peak at the LL side while  $|\Psi_A(x_1, x_2, 0)|^2$  at the RR side. It is, however, not the case

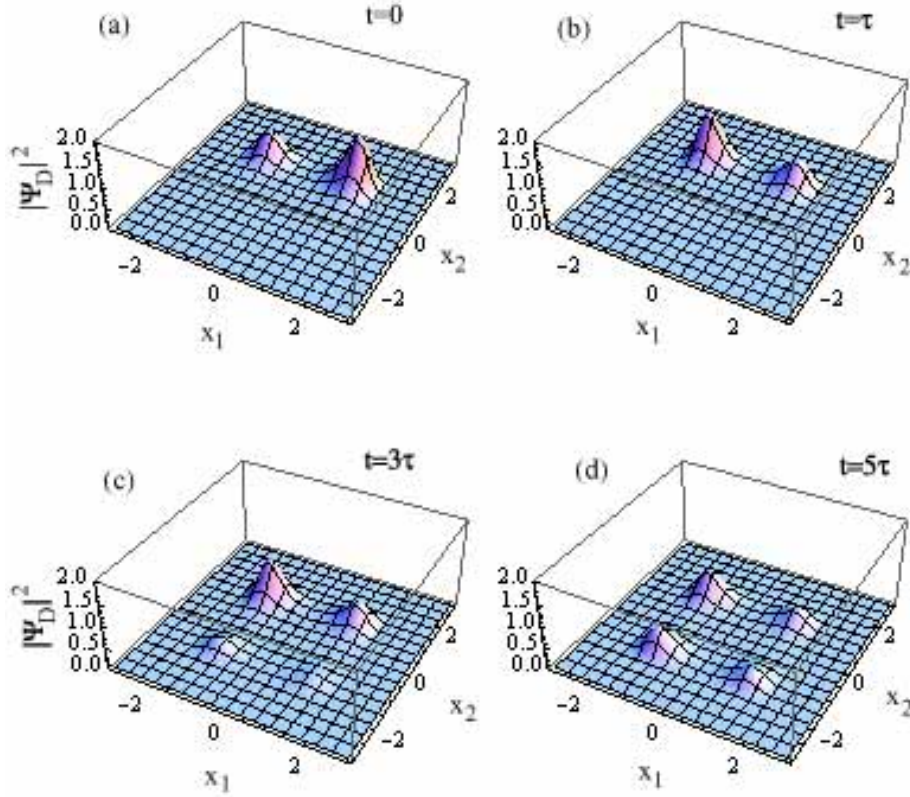


FIG. 12: (Color online) Magnitudes of  $|\Psi_D(x_1, x_2, t)|^2$  of the wavepacket D with  $g = 0.1$  at (a)  $t = 0$ , (b)  $t = \tau$ , (c)  $t = 3\tau$  and (d)  $t = 5\tau$ ,  $\Psi_D(x_1, x_2, t)$  at  $t = \tau, 3\tau$  and  $5\tau$  being orthogonal to  $\Psi_D(x_1, x_2, 0)$ .

for the wavepacket D. Magnitudes of wavefunctions  $|\Psi_D(x_1, x_2, t)|^2$  for  $g = 0.1$  at  $t = 0.0, \tau, 3\tau$  and  $5\tau$  ( $\tau = 11.02$ ) are plotted in Figs. 12(a)-12(d), respectively, where all wavefunctions in Figs. 12(b), 12(c) and 12(d) are orthogonal to that in Fig. 12(a).

### C. The $g$ dependence of $\tau$ and $\tau_{min}$

Although calculations in the preceding subsection Sec. III B have been reported only for  $g = 0.0, 0.1$  and  $0.2$ , we may repeat calculations of the orthogonality time  $\tau$  by changing  $g$  for the four wavepackets. Calculated  $\tau$  is plotted as a function of  $g$  by dashed curves in Figs. 13(a)-13(d). Obtained  $\tau$  for the four wavepackets is expressed in the second column of Table 2, whose third and fourth columns show  $C_{av}^2$  and  $C(0)^2$ , respectively,  $E_\nu$  ( $\nu = 0 - 3$ ) and  $\theta$

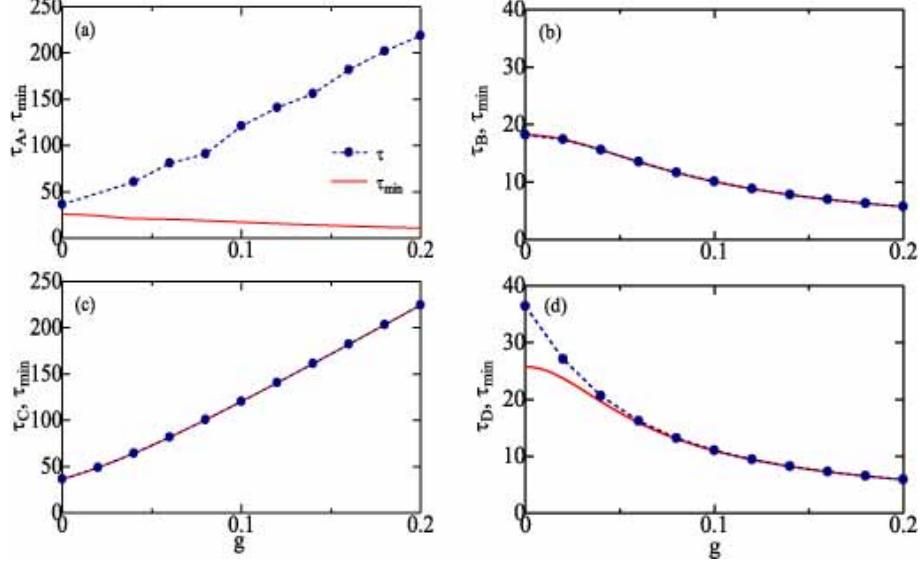


FIG. 13: (Color online) The  $g$  dependence of the orthogonality time  $\tau$  (dashed curves) and minimum values  $\tau_{min}$  (solid curves) for (a) wavepacket A, (b) B, (c) C and (d) D.

being  $g$  dependent [Eqs. (12)-(15), (22)]. Figures 13(a)-13(d) show that with increasing  $g$ ,  $\tau_A$  and  $\tau_C$  are increased, while  $\tau_B$  and  $\tau_D$  are decreased. This is because with increasing  $g$ , a gap of  $E_1 - E_0$  is decreased whereas  $E_3 - E_0$  and  $E_2 - E_0$  are increased (Fig. 2).

wavepacket	$\tau$	$C_{av}^2$	$C(0)^2$
A	$\simeq \frac{\pi\hbar}{(E_1-E_0)}$	$\frac{1}{8}(4 - \sin^2 2\theta) - \frac{1}{2} \delta(g)$	$\frac{1}{4}(1 - \cos 2\theta)^2$
B	$\frac{\pi\hbar}{(E_3-E_0)}$	$1 - \frac{1}{2} \sin^2 2\theta$	$\cos^2 2\theta$
C	$\frac{\pi\hbar}{(E_1-E_0)}$	$\frac{1}{4}(1 + \sin^2 2\theta)$	$\frac{1}{4}(1 - \sin 2\theta)^2$
D	$\frac{\pi\hbar}{(E_2-E_0)}$	$\frac{1}{8}(3 - \sin^2 2\theta) - \frac{1}{8} \delta(g)$	$\frac{1}{4} \cos^2 2\theta$

Table 2 Calculated  $\tau$ ,  $C_{av}^2$  and  $C(0)^2$  for four wavepackets A, B, C and D.

We may evaluate the minimum orthogonality time  $\tau_{min}$  of our DW model, calculating the expectation energy  $E$  and its root-mean-square value  $\Delta E$  in Eq. (1), which are expressed by

$$E = \sum_{\nu} |a_{\nu}|^2 (E_{\nu} - E_0) = |a_1|^2 \Omega_1 + |a_2|^2 \Omega_2 + |a_3|^2 \Omega_3, \quad (63)$$

$$(\Delta E)^2 = \sum_{\nu} |a_{\nu}|^2 (E_{\nu} - E_0)^2 - E^2 = |a_1|^2 \Omega_1^2 + |a_2|^2 \Omega_2^2 + |a_3|^2 \Omega_3^2 - E^2. \quad (64)$$

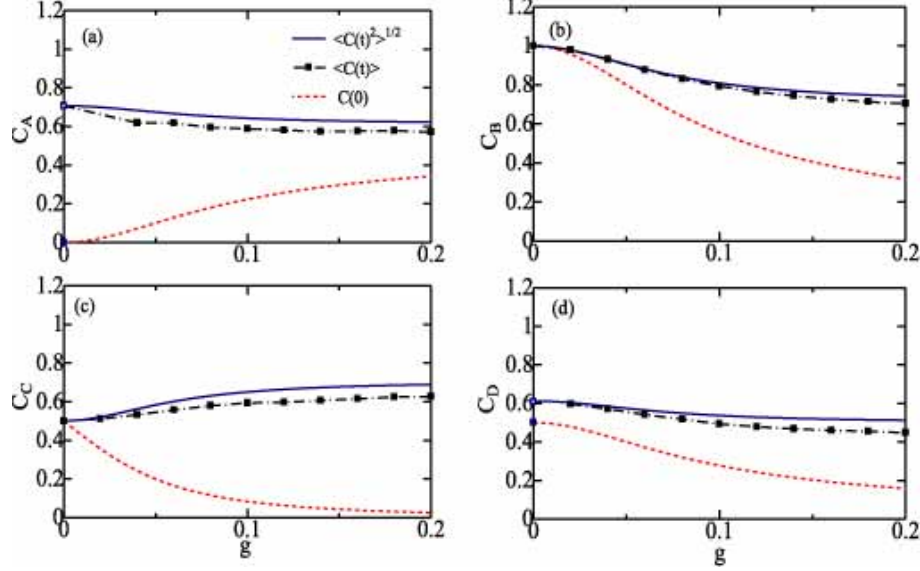


FIG. 14: (Color online) The  $g$  dependence of averaged concurrences,  $C_{av} [= \sqrt{\langle C(t)^2 \rangle}]$  (solid curves) and  $\langle C(t) \rangle$  (chain curves), and of the initial concurrence  $C(0)$  (dashed curves) for (a) wavepacket A, (b) B, (c) C and (d) D.

Solid curves in Figs. 13(a)-13(d) express  $\tau_{min}$  calculated by Eqs. (1), (63) and (64) as a function of  $g$  for four wavepackets A-D. With increasing  $g$ ,  $\tau_{min}$  increases for the wavepacket C, whereas those for wavepackets A, B and D decrease. The ratio of  $\tau/\tau_{min}$  is unity for wavepackets B and C in Figs. 13(b) and 13(c). However, we obtain  $\tau/\tau_{min} = 1.414$  and  $1.0$  for  $g = 0.0$  and  $g \gtrsim 0.06$ , respectively, for the wavepacket D in Fig. 13(d). Furthermore, this ratio more apparently exceeds unity for the wavepacket A in Fig. 13(a) where  $\tau/\tau_{min} = 1.414, 7.00$  and  $20.0$  for  $g = 0.0, 0.1$  and  $0.2$ , respectively. This is accounted for by the fact that with increasing  $g$ ,  $\tau$  is increased because of a narrowed energy gap of  $E_1 - E_0$  while  $\tau_{min}$  is decreased by a high-energy contribution of  $E_3 - E_0$  to  $E$  (Fig. 2).

#### D. $g$ dependence of $C_{av}$ and $C(0)$

We may calculate  $C_{av}$  and  $C(0)$  of the four wavepackets as a function of  $g$ , whose results are plotted in Figs. 14(a)-14(d). In the wavepacket A,  $C_{av}$  has a discontinuity at  $g = 0.0$  as mentioned before:  $C_{av} = 0.0$  and  $0.707$  at  $g = 0$  and  $0_+$ , respectively. When  $g$  is introduced,  $C(0)$  is increased from zero while  $C_{av}$  is decreased from  $0.707$  [Fig. 14(a)]. In

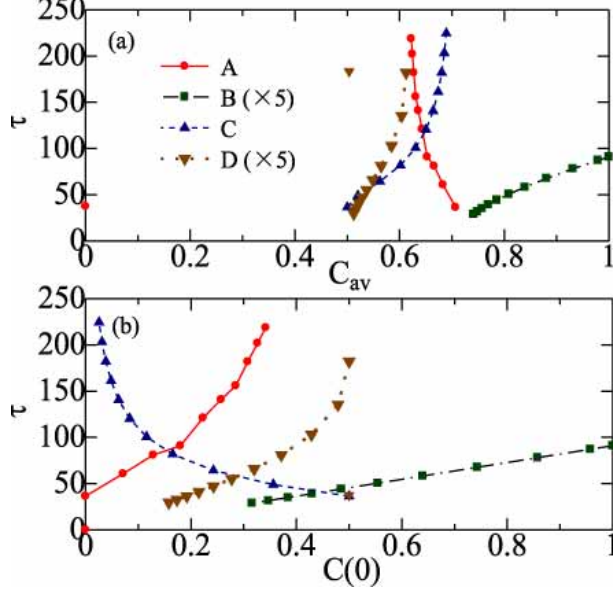


FIG. 15: (Color online) (a)  $C_{av}$  vs.  $\tau$  and (b)  $C(0)$  vs.  $\tau$  for wavepackets A (circles), B (squares), C (triangles) and D (inverted triangles),  $\tau$  for wavepackets B and D being multiplied by a factor of five. In (a), a point at  $(C_{av}, \tau) = (0.0, 36.40)$  for the wavepacket A is separated from that at  $(0.706, 36.40)$  because of the discontinuity of  $C_{av}$  at  $g = 0.0$  (Fig. 14). Similarly, a point at  $(C_{av}, \tau) = (0.5, 36.40)$  for the wavepacket D is separated from that at  $(0.6124, 36.40)$ .

the wavepacket B, both  $C_{av}$  and  $C(0)$  are gradually decreased with increasing  $g$  [Fig. 14(b)]. On the contrary, in the wavepacket C,  $C_{av}$  is increased from 0.5 but  $C(0)$  is decreased from 0.5 when  $g$  is introduced [Fig. 14(c)]. In the wavepacket D,  $C_{av}$  has a discontinuity at  $g = 0.0$ :  $C_{av} = 0.5$  and  $0.612$  at  $g = 0$  and  $0_+$ , respectively, and both  $C_{av}$  and  $C(0)$  are decreased with increasing  $g$  [Fig. 14(d)].

Chain curves in Figs. 14(a)-14(d) show  $\langle C(t) \rangle$  for the four wavepackets, which are nearly in agreement with  $C_{av} (= \sqrt{\langle C(t)^2 \rangle})$  plotted by solid curves.

### E. The dependence of $\tau$ on $C_{av}$ and $C(0)$

Comparing Figs. 13(a)-13(d) and Figs. 14(a)-14(d), respectively, we may examine the relation between the orthogonality time ( $\tau$ ) and the concurrence ( $C_{av}$  or  $C(0)$ ). Figures 15(a) and 15(b) show the  $C_{av}$  vs.  $\tau$  plot and the  $C(0)$  vs.  $\tau$  plot, respectively. For wavepackets B and D (squares and inverted triangles),  $\tau$  is increased with increasing  $C_{av}$  or  $C(0)$ . We

note, however, that  $\tau$  of the wavepacket A (circles) is increased with increasing  $C(0)$  but with decreasing  $C_{av}$ . On the contrary,  $\tau$  of the wavepacket C (triangles) is increased with increasing  $C_{av}$  but with decreasing  $C(0)$ . Figures 15(a) and 15(b) imply that the effect of  $C_{av}$  on  $\tau$  is generally different from that of  $C(0)$  and that when the concurrence is increased, the orthogonality time may be increased or decreased, depending on the adopted wavepacket. This is in contrast with Refs. [4, 6, 7] but in agreement with Refs. [5, 8, 10].

#### IV. CONCLUDING REMARK

Batle *et al.* [6] and Curilef *et al.* [7] studied two uncoupled qubits with eigenvalues

$$E_0 = 0, \quad E_1 = E_2 = \epsilon_1, \quad E_3 = 2\epsilon_1, \quad (65)$$

where  $\epsilon_1$  stands for an energy of a free qubit. For wavepackets with  $|a_0|^2 = |a_3|^3 \neq 0.0$ , the ratio of  $\tau/\tau_{min}$  is shown to be unity for a maximally entangled state and  $\sqrt{2}$  for a separate state [6, 7]. In our wavepackets A, B and D with  $a_3 = a_0 \neq 0.0$  for  $g = 0.0$ , the ratio is  $\tau/\tau_{min} = 1.0$  in the wavepacket B while it is  $\sqrt{2}$  in wavepackets A and D, which are consistent with results of Refs. [6, 7]. However, in the wavepacket C with  $a_3 = 0.0$ , which corresponds to the *singular* case after Chau [9], we obtain  $\tau/\tau_{min} = 1.0$  for  $g = 0.0$  although it is not a maximally entangled state ( $C = 0.5$ ), in agreement with Ref. [9].

Zander *et al.* [10] adopted two interacting qubits given by the Hamiltonian

$$H = \hbar\omega_0[2I^{(1)} \otimes I^{(2)} - \sigma_x^{(1)} \otimes I^{(2)} - I^{(1)} \otimes \sigma_x^{(2)}] + \hbar\omega[I^{(1)} \otimes I^{(2)} - \sigma_x^{(1)} \otimes \sigma_x^{(2)}], \quad (66)$$

where  $\omega_0$  expresses the energy of free qubits,  $\omega$  stands for the interaction,  $I$  is the identity matrix and  $\sigma_x$  is the  $x$ -Pauli matrix. Eigenvalues of the Hamiltonian are [10]

$$E_0 = 0, \quad E_1 = E_2 = 2\hbar(\omega + \omega_0), \quad E_3 = 4\hbar\omega_0. \quad (67)$$

Ref. [10] studied effects of entanglement on the evolution speed in interacting two qubits, evaluating the linear entropy mainly for the three cases of  $\omega = \omega_0$ ,  $\omega_0 = 0$  and  $\omega = 3\omega_0$  with arbitrary expansion coefficients  $\{a_\nu\}$  for wavepackets. The study of Ref. [10] is complementary to ours in which calculations have been made for an arbitrary interaction  $g$  with four sets of expansion coefficients  $\{a_\nu\}$  for wavepackets A-D. It was claimed in Ref. [10] that with the exception of some *special* cases, states with a small initial entanglement tend

to evolve in the fastest way in coupled qubits. This is not inconsistent with our result of the wavepacket A showing that  $\tau/\tau_{min} = 7.00$  and  $20.0$  for  $C(0) = 0.223$  and  $0.342$ , respectively. However, we obtain  $\tau/\tau_{min} = 1.0$  almost independently of  $C(0)$  in wavepackets B, C, and D (Figs. 13 and 14), which might correspond to special cases after Ref. [10]. Refs. [4] and [10] explained that for  $\tau$  to reach the bound, it is necessary to have either an initial entangled state, or an interaction term capable of creating entanglement. This seems not to be applicable to the wavepacket A for which  $\tau/\tau_{min} = 20.0 \gg 1.0$  even if  $C(0) = 0.342$  for  $g = 0.2$  (Figs. 13 and 14). This disagreement might arise from a difference in models adopted in Ref. [10] and the present study: the interaction dependence of eigenvalues in Eq. (67) are different from that in Eqs. (12)-(15).

In the simple case, we may obtain an analytical expression for  $\tau$  expressed in terms of  $C_{av}$  and/or  $C(0)$ . Indeed, for the wavepacket B, a calculation with Eqs. (22), (51) and (52) leads to

$$\tau_B = \tau_{min} = \left(\frac{\pi}{2\delta}\right) \sqrt{2C_{av}^2 - 1} = \left(\frac{\pi}{2\delta}\right) C(0), \quad (68)$$

which is numerically confirmed in Fig. 15. Unfortunately it is impossible to obtain analytical results for wavepackets A, C and D.

In summary, we have studied dynamical properties of four wavepackets A, B, C and D (Table 1), by using an exactly solvable coupled DW system described by Razavy's potential [12]. Our model calculations yield the followings:

- (1) The correlation function  $\Gamma(t)$  and concurrence  $C(t)$  in interacting two qubits show complicated and peculiar time dependence (Figs. 4-11),
- (2) The quantum evolution speed measured by  $\tau^{-1}$  is not necessarily increased by an introduced interaction  $g$ : *e.g.* it is decreased in wavepackets A and C (Fig. 13),
- (3) The concurrence,  $C_{av}$  or  $C(0)$ , may be decreased by an increased interaction (Fig. 14),
- (4) The relation between  $C(0)$  and  $\tau$  is generally not the same as that between  $C_{av}$  and  $\tau$ , and the evolution speed may be increased or decreased with the increased concurrence ( $C_{av}$  or  $C(0)$ ), depending on a wavepacket (Fig. 15), and
- (5)  $\tau$  may not reach its minimum value  $\tau_{min}$  even when the entanglement is present in coupled DW systems.

Items (4) and (5) are in contrast with the non-interacting case where  $\tau$  is decreased with increasing  $C(0)$  and the ratio  $\tau/\tau_{min}$  approaches unity in entangled state [4-8]. Items (4) and

(5) suggest that the relation between the evolution speed and the entanglement in coupled qubits is not definite in contrast to that in uncoupled case [4–8]. In the present study, we do not take into account environmental effects which are expected to play important roles in real DW systems. An inclusion of dissipative effects is left as our future subject.

## Acknowledgments

This work is partly supported by a Grant-in-Aid for Scientific Research from Ministry of Education, Culture, Sports, Science and Technology of Japan.

- 
- [1] M. J. Storcz and F. K. Wilhelm, Phys. Rev. A **67** (2003) 042319.
  - [2] N. Margolus and L. B. Levitin, Physica D **120** (1998) 188.
  - [3] L. Mandelstam and I. G. Tamm, J. Phys. USSR **9** (1945) 249; K. Bhattacharyya, J. Phys. A **16** (1983) 2993; P. Pfeifer, Phys. Rev. Lett. **70** (1993) 3365.
  - [4] V. Giovannetti, S. Lloyd, and L. Maccone, Europhys. Lett. **62** (2003) 615.
  - [5] V. Giovannetti, S. Lloyd, and L. Maccone, Phys. Rev. A **67** (2003) 052109.
  - [6] J. Batle, M. Casas, A. Plastino, and A. R. Plastino, Phys. Rev. A **72** (2005) 032337.
  - [7] S. Curilef, C. Zander and A. R. Plastino, Eur. J. Phys. **27** (2006) 1193.
  - [8] A. Borrás, M. Casas, A. R. Plastino, and A. Plastino, Phys. Rev. A **74** (2006) 022326.
  - [9] H. F. Chau, Phys. Rev. A **82** (2010) 056301.
  - [10] C. Zander, A. Borrás, A. R. Plastino, A. Plastino, and M. Casas, J. Phys. A **46**, 095302 (2013).
  - [11] D. J. Tannor, *Introduction to quantum mechanics: A time-dependent perspective* (Univ. Sci. Books, Sausalito, California, 2007).
  - [12] M. Razavy, Am. J. Phys. **48** (1980) 285.
  - [13] F. Finkel, F. Finkel, A. Gonzalez-Lopez and M. A. Rodriguez, J. Phys. A **32** (1999) 6821.
  - [14] B. Bagchi and A. Ganguly, J. Phys. A **36** (2003) L161.
  - [15] The energy and time are measured in units of  $|V(0)|/2$  and  $2\hbar/|V(0)|$ , respectively, in this study.
  - [16] W. K. Wootters, Quan. Inf. Comp. **1** (2001) 27.



[17] In the wavepacket A, one term in  $\langle C_A(t)^2 \rangle$  leads to  $(1/t_f) \int_0^{t_f} \cos(\Omega_3 - 2\Omega_1)t \, dt = [\sin(\Omega_3 - 2\Omega_1)t_f]/[(\Omega_3 - 2\Omega_1)t_f] \propto \delta(\Omega_3 - 2\Omega_1)$  which yields the delta-function contribution at  $g = 0$  where  $\Omega_3 - 2\Omega_1 = 0$ . The situation is similar to the wavepacket D in which  $\Omega_2 - \Omega_1 = 0$  at  $g = 0$ .